SUPERPLUME FORMATION ON MARS FOLLOWING A GIANT IMPACT. R. I. Citron[1] and M. Manga[1], [1]Department of Earth and Planetary Sci., University of California, Berkeley, CA 94720 (ricitron@berkeley.edu).

Introduction: Mars likely experienced a giant impact ~4.5 Ga [1]. Such an impact would have excavated a significant fraction of ancient crust, and is the likely initial origin of the ~5 km difference in surface elevation and ~26 km difference in crustal thickness between the north and south hemispheres, also known as the Mars crustal dichotomy or Borealis basin [2,3]. However, it has also been suggested that the crustal dichotomy formed as a result of a superplume [4], which could potentially explain the pattern of remanent crustal magnetism is Mars' southern hemisphere [5] and the formation of Tharsis on the dichotomy boundary [6,7]. Because both a giant impact and a superplume can explain features prevalent on early Mars, we investigate a possible causal relationship between the two processes, specifically if a superplume could naturally develop as a result of a giant impact [8].

We propose that a giant impact in one hemisphere induced superplume formation in the opposite hemisphere (Fig. 1). In this scenario, a giant impact excavated a significant fraction of ancient crust in the present-day northern hemisphere. While a new northern crust would form relatively rapidly, it would form from an already depleted mantle (depleted from forming the original crust) and thus be depleted in radiogenic-heat producing elements relative to the older, more enriched southern crust [9,10]. Transient upwellings under the impact site would dissipate over longer timescales (10s to 100s of Myr), when the dominant upwelling(s) would migrate under the thicker, insulating crust in the southern hemisphere. Melt generation from the upwelling(s) would further thicken the southern crust. To investigate our hypothesis for the interior evolution of Mars following a giant impact, we conduct 3D simulations of mantle convection for various post-impact scenarios.

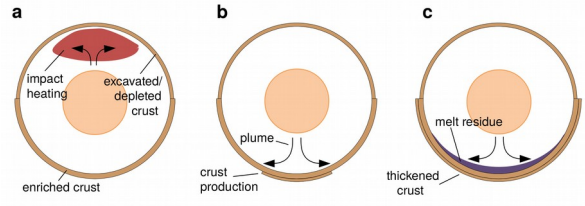

Figure 1. A giant impact causes excavation, heating, and a transient upwelling in the northern hemisphere (a), resulting in a superplume forming under the thicker, enriched southern crust (b). This enhances the initial crustal variation produced by the impact, and forms melt residue (c).

Methods: Mantle convection simulations are conducted using the CitcomS mantle convection code [11,12]. We use the Boussinesq approximation with parameters similar to [4], but with a variable internal heating rate based on [13], ΔT=1600K, and a Rayleigh number of 10^8. A southern crust of thickness $d_{cr,S}$ is parameterized by a reduction of thermal conductivity κ by a factor κ_{ins} and/or an enrichment in heat production Q by a factor $Q_{ER,S}$. In some cases, a northern crust is included and similarly parameterized by $d_{cr,N}$ and $Q_{ER,N}$, in addition to a depletion of mantle material by a factor Q_{DE}. In two cases, an initial temperature perturbation based on impact heating from a projectile of radius R_i is included [14] to examine the effect of initial post-impact transient upwellings on the long-term convective state. We also track melt production using a tracer method [15], incorporating the effect of latent heat during melt production.

Results: Table 1 shows results for seven simulations. We report the time until single-plume convection is reached, t_{SP}, based on when a clear single plume is visible extending through the entire mantle, centered under the insulating crust in the southern hemisphere. Run 0 is a control case with no crust that never achieves single plume convection.

Table 1: Simulation results

Run	$d_{cr,S}$ (km)	$d_{cr,N}$ (km)	$Q_{ER,S}$	$Q_{ER,N}$	κ_{ins}	R_i (km)	t_{SP} (Myr)
0	-	-	-	-	-	-	Never
1	50	-	4	4	0.75	-	59
2	50	-	4	4	-	-	60
3	25	-	4	4	0.75	-	60
4	50	25	10	4	-	-	61
5	50	25	10	10	-	-	Never
6	50	-	4	4	0.75	600	60
7	50	-	4	4	0.75	1200	89

We find that the inclusion of an enriched crust in the southern hemisphere can induce single plume convection on relatively short timescales (<100 Myr), even with no reduction of thermal diffusivity in the crust (Run 2) or with a thinner initial southern crust (Run 3). When a thinner, less enriched crust is included for the northern hemisphere a superplume still develops under the more heavily enriched southern crust (Run 4), whereas no superplume develops in a

control case (Run 5) where both hemispheres have the same factor of enrichment in the crust (Fig. 2). Even when an initial post-impact temperature perturbation is included in the northern hemisphere (Runs 6 and 7), the upwelling(s) eventually migrate under the more enriched southern crust (Fig. 3).

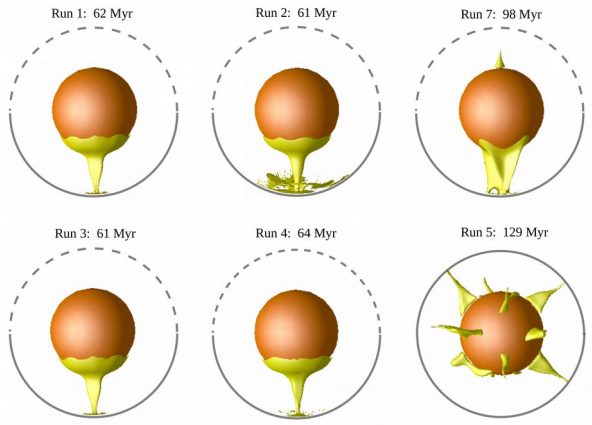

Figure 2. Upwelling contours for residual temperature of 80K, with the upper 100km omitted for clarity. The southern crust (solid grey line) is enriched in radiogenic-heat producing elements relative to the northern crust (dashed grey line). After <100 Myr a superplume develops under the enriched southern crust. In Run 5, the northern and southern crust have the same degree of enrichment and no superplume develops.

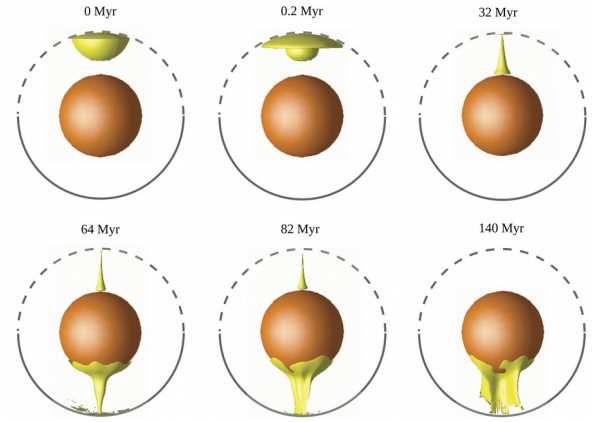

Figure 3. Evolution of Run 6 over time. The simulation begins with a temperature perturbation from a giant impact in the northern hemisphere, which quickly dissipates. Over time, a superplume develops under the more enriched southern crust.

Discussion and Future Work: Our results show that a giant impact on early Mars can strongly influence the subsequent convective pattern. The primary driver of the mantle flow is the distribution of radiogenic-heat producing elements in the crust. If one hemisphere of the planet contains a crust that is more enriched in radiogenic-heat producing elements, then a superplume develops under the enriched crust [8].

The amount of additional melt produced by the superplume is consistent with crustal thickness estimates [8], and may explain the stronger remanent magnetism observed in Mars' southern hemisphere. While a giant impact would have likely erased any prior remanent magnetic signatures, the unique lineations of opposite polarity observed in the remanent magnetic signatures could result from crust production spreading from a superplume center [5].

Superplume formation on early Mars may also be linked to the formation of Tharsis on the dichotomy boundary. Plume migration from the south pole to Tharsis' location is supported by observations of volcanic resurfacing, demagnetization, and increased crustal thickness along that path [16,17]. If the large upwelling under the southern crust causes significant melting, it could potentially result in sufficient melt residue to induce plume migration or lithospheric rotation, resulting in the formation of Tharsis on the dichotomy boundary [6,7]. The timescale of superplume formation (~100 Myr) is sufficient to allow for additional melting and plume migration between dichotomy formation ~4.5 Ga and the emplacement of Tharsis ~3.7 Ga [18,19]. In future work, we will further explore the effect of melt production on plume migration.

Acknowledgments: Supported by NASA 17-SSW17-0130.

References: [1] Bottke W. F. and Andrews-Hanna J. C. (2017) *Nat Geosci.*, 10, 344–348. [2] Marinova M. M. et al. (2008) *Nature*, 453, 1216-1219. [3] Andrews-Hanna J. C. et al. (2008) *Nature*, 453, 1212–1215. [4] Roberts J. H. and Zhong S. (2006) *JGR Planets*, 111, E06013. [5] Citron R. I. and Zhong S. (2012) *PEPI*, 212–213, 55–63. [6] Zhong S. (2009) *Nat Geosci.*, 2, 19–23. [7] Šrámek O. and Zhong S. (2010), *JGR Planets*, 115, E09010. [8] Citron R. I. et al. (2018) *EPSL*, 491, 58–66. [9] Thiriet M. et al. (2018) *JGR Planets*, 123, 823-848. [10] Ruedas T. and Breuer D. (2017) *JGR Planets*, 122, 1554–1579. [11] Zhong S. et al. (2000) *JGR Solid Earth*, 105, 11063–11082. [12] Tan E. et al. (2006) *G3*, 7. [13] Lodders K. and Fegley B. (1997) *Icarus*, 126, 373–394. [14] Golabek G. J. et al. (2011) *Icarus*, 215, 346–357. [15] Li M. et al. (2016) *G3*, 17, 2884–2904. [16] Hynek B. M. et al. (2011) *EPSL*, 310, 327–333. [17] Cheung K. K. and King S. D. (2014) *JGR Planets*, 119, 1078–1085. [18] Anderson R. C. et al. (2001) *JGR Planets*, 106, 20563–20585. [19] Bouley S. et al. (2018) *EPSL*, 488, 126–133.